Materials Letters 361 (2024) 136152

Contents lists available at ScienceDirect

Materials Letters

journal homepage: www.elsevier.com/locate/matlet

Assessment of the biocompatibility and bioimaging potential of fluorescent carbon dots derived from waste biomass

Dinesh K. Patel [a], So-Yeon Won [a], Eunseo Jung [a], Sayan Deb Dutta [b], Tejal V. Patil [b], Ki-Taek Lim [b], Sung Soo Han [a,*]

[a] School of Chemical Engineering, Yeungnam University, 280-Daehak-ro, Gyeongsan 38541, South Korea
[b] Department of Biosystems Engineering, Institute of Forest Science, Kangwon National University, Chuncheon 24341, South Korea

ARTICLE INFO

Keywords:
Banana peels
Carbon dots
Cytotoxicity
Bioimaging

ABSTRACT

The fluorescent carbon dots (C-dots) are attractive platforms in bioimaging, biosensing, and disease detection applications due to their attractive physicochemical characteristics. Herein, we synthesized fluorescent and biocompatible C-dots from banana biomass through heat treatment. The C-dots were soluble in water and showed a fluorescent behavior under UV light (365 nm). The synthesized C-dots demonstrated an excitation-dependent emission behavior with a satisfying quantum yield of 15 %. The C-dots exhibited different functional groups in their structure. The C-dots have no adverse effects on human dermal fibroblast cells (HDFs), indicating their biocompatibility. The C-dots have successfully delivered inside cells and showed fluorescent behavior. These results showed that the prepared materials could potentially explore high-performance bioimaging applications.

1. Introduction

Carbon dots (C-dots), a zero-dimensional (0D) carbon nanomaterial with a diameter <10 nm, have emerged as an attractive nanomaterial for bioimaging, biosensing, and disease detection applications owing to their better solubility in aqueous conditions, low cytotoxicity, excitation dependent emission, and biocompatibility. The carbon quantum dots and graphene quantum dots are two major C-dots. Graphene quantum dots are small fragments of single or few layers of graphene sheets, whereas carbon quantum dots have crystal lattices, exhibiting the luminescence and quantum confinement effects [1]. The pure and surface-functionalized C-dots synthesized from different sources exhibited great potential in imaging different bacterial, and animal cells. Different approaches, including microwave heating, hydrothermal, laser ablation, electrochemical oxidation, combustion, and arc discharge, have been explored in synthesizing C-dots for different applications [2]. However, most discussed methods require a post-treatment process or expensive raw materials to synthesize fluorescent and biocompatible nanomaterials. Therefore, an effective approach is necessary to synthesize the value-added C-dots from waste sources without using toxic solvents or a post-purification process. Photoluminescence (PL) is one of the fascinating characteristics of C-dots and is widely affected by the precursor properties, synthesis method, conditions, and purification process [3]. The PL properties of C-dots can be altered by incorporating heteroatoms, including nitrogen, oxygen, sulfur, and phosphorous, and grafting with other chemical functionalities. Feng and coworkers synthesized C-dots with tunable photoluminescence properties through a deep eutectic solvent prepared from sulfuric acid and quaternary ammonium salt. The developed C-dots contained different heteroatoms, such as N, O, and S, in their structure and exhibited good PL characteristics. Oxygen species on C-dots can reduce the band gap between the highest occupied molecular orbital and the lowest occupied molecular orbital, resulting in the red shifting in emission wavelength [4]. Mostly, organic molecules have been explored in synthesizing fluorescence C-dots with good quantum yield through the hydrothermal method due to its easy processability [5]. However, the cytotoxicity of the organic moieties restricts the broad applicability of the synthesized nanomaterials. Different sources, such as biomass, vegetable, and fruit peels, have been explored as precursor moieties due to their non-toxic, cost-effective, easy availability, and biocompatibility. Atchudan and coworkers previously synthesized C-dots using waste banana peels through the hydrothermal method (200 °C, & 24 h) for biological applications. They used an ammonium solution to insert the nitrogen heteroatom in the structure of the C-dots to enhance the fluorescence behavior [6].

* Corresponding author.
E-mail address: sshan@yu.ac.kr (S. Soo Han).

https://doi.org/10.1016/j.matlet.2024.136152
Received 22 October 2023; Received in revised form 26 December 2023; Accepted 12 February 2024
Available online 13 February 2024

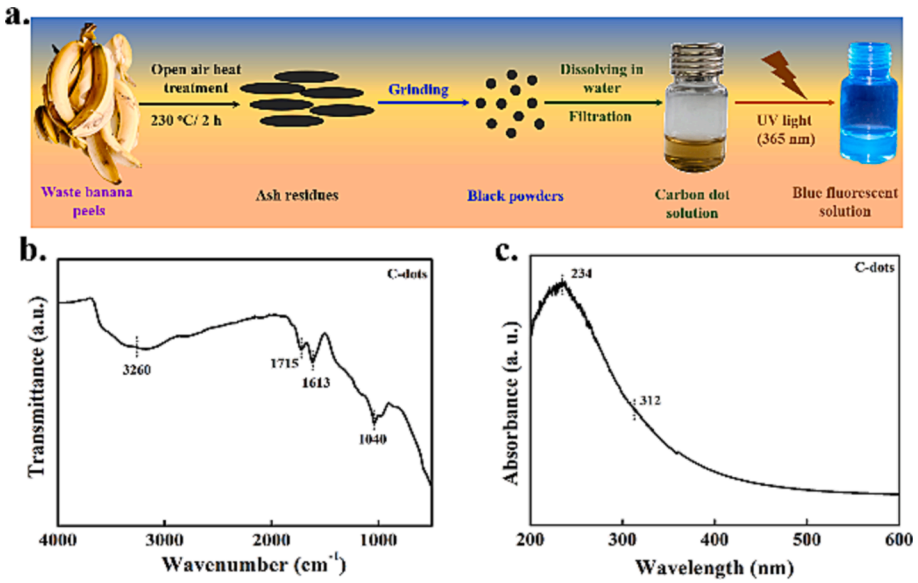

Fig. 1. **(a)** Schematic presentation for the synthesis of biocompatible and fluorescent C-dots from waste banana peels through heat treatment, **(b)** FTIR, and **(c)** UV–visible spectrum of the C-dots.

Thus, developing chemically functionalized and biocompatible C-dots through a simple process from waste material is desirable for biological applications. Herein, we synthesized fluorescent and biocompatible C-dots using waste banana peels through heat treatment for bioimaging applications. The C-dots have no adverse effects on HDF cells and are easily translocated inside cells with intense fluorescence characteristics, which can be explored in high-performing cell imaging applications.

2. Materials and methods

2.1. Synthesis of C-dots

The synthesis of fluorescent C-dots from waste banana peels was performed through heat treatment. Briefly, the fresh peels were carbonized at 240 °C for 2 h, followed by grinding and filtration. The filtrate was centrifuged (10000 RPM, 15 min), and the supernatant was collected for dialysis against distilled water for 3 days. The obtained material was freeze-dried for further applications. The characterization process is given in the **supplementary Section (SI)** of the manuscript.

2.2. Cytotoxicity and bioimaging

For this, 1×10^4 HDF cells were mixed with different C-dot concentrations (0, 25, 50, 100, and 150 μg/mL) in 96-well plates and incubated for 24 h in a 5 % CO_2 incubator at 37 °C. The groups without C-dots were considered as controls. After incubation, WST-8 dye (10 μL) was added to the cultured media and incubated for 2 h to form the formazan. The absorbance was measured with a spectrophotometer at 450 nm. All experiments were done in triplicate (n = 3). Statistical significance was taken at $^*p < 0.05$. For bioimaging, 0.5×10^4 cells were treated with C-dots (25 μg/mL) for different periods, followed by washing with PBS. Then, cells were stained with 5 μL of DiO dye in media and incubated at 37 °C for 10–15 min. The cells were washed with PBS and fixed with 3.7 % paraformaldehyde, and images were captured using an inverted Fluorescence microscope. The primary culture process of cells is given in the **SI** of the manuscript.

3. Results and discussion

The schematic presentation of synthesizing fluorescent C-dots from waste banana peels is presented in (Fig. 1**a**). The synthesized C-dots were easily soluble in water, and images of water-solubilized C-dots under different conditions (normal and UV light) are also shown in (Fig. 1**a**). An intense blue color was observed under the irradiation of UV light (365 nm), demonstrating the fluorescence characteristic of the synthesized material. The FTIR spectrum C-dots is given in (Fig. 1**b**). The synthesized C-dots show the characteristics of absorption peaks at 3260, 1715, 1613, and 1040 cm^{-1} for hydroxyl stretching (–OH), carbonyl vibration (C═O), graphitic carbon (C═C), and C–O vibration, respectively. This finding demonstrated that the synthesized C-dots have

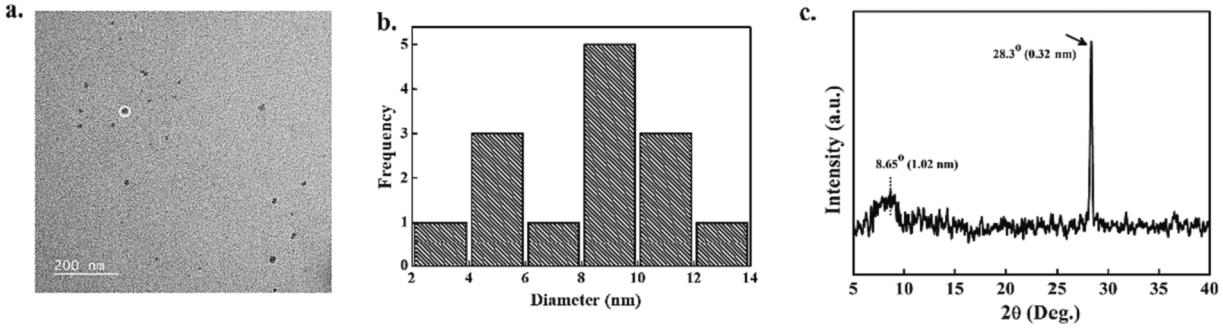

Fig. 2. The morphological assessment of the synthesized C-dots. **(a)** FE-TEM image of C-dots (white circle indicates the nearly spherical morphology), **(b)** The histogram of the C-dots, and **(c)** The XRD pattern of the synthesized C-dots.

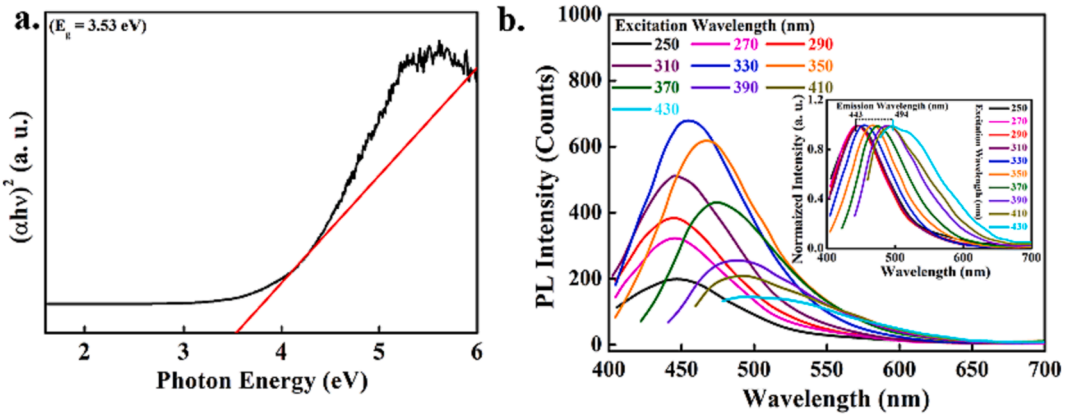

Fig. 3. **(a)** Tauc plot for the assessment of the bandgap energy, and **(b)** PL spectra of the synthesized C-dots at different excitation wavelength (inset normalized emission spectra).

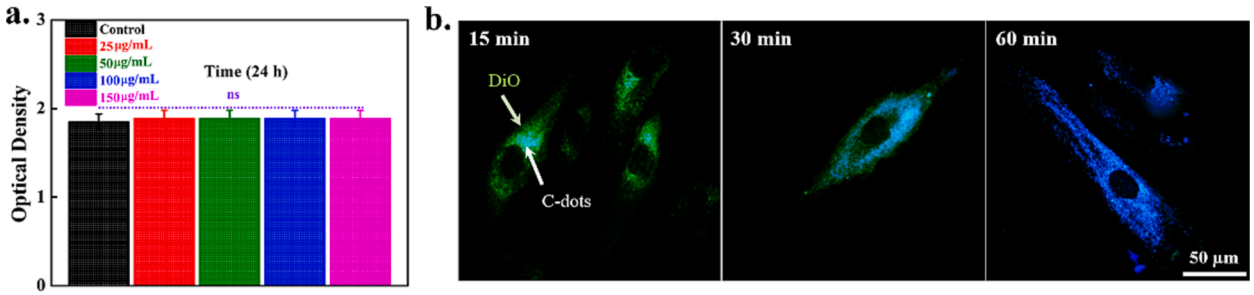

Fig. 4. Biocompatibility evaluation of the synthesized C-dots. **(a)** HDFs viability data with C-dots at different concentrations after 24 h of incubation, and **(b)** Cell imaging results at indicated periods.

abundant polar functional groups on their surface. The UV–visible spectrum of the synthesized C-dots is presented in (Fig. 1**c**). The C-dots show strong absorption and shoulder peaks at 234 and 312 nm, which can be attributed to the π–π* transition of the C═C moieties and n– π* transition of C═O bonds, respectively [7]. These findings further suggested the existence of oxygenated functional groups in the C-dots, as observed in the FTIR result. The morphological examination of the C-dots was assessed by using FE-TEM, and the image is shown in (Fig. 2**a**). The C-dots were nearly spherical with an average diameter of 8.25 ± 0.65 nm. The histogram profile of C-dots is also presented in (Fig. 2**b**). The particle size distribution has occurred within the 3.60–13.03 nm range. The surface charge of the C-dots was measured in terms of zeta potential, and it was −35.8 ± 1.79 mV, demonstrating the presence of some charged functional groups as observed in the FTIR result. It is well-known that carboxyl, sulfonate, sulfate, phosphonate, and phosphate generate negative zeta potential for synthesized C-dots. The XRD analysis was performed to assess the structural characteristics of the synthesized C-dots, and the obtained pattern is shown in (Fig. 2**c**). The C-dots show broad and sharp diffraction peaks at 8.65° (100) and 28.3° (002) with corresponding interlayer distances of 1.02, and 0.32 nm, respectively, demonstrating the functionalized characteristics of graphitic sheets. The bandgap energy (E_g) between the valence band and conduction band of the prepared C-dots was calculated from the UV–visible spectrum of nanomaterial through a Tauc plot, and the result is shown in (Fig. 3**a**). The value was 3.53 eV, and less than the intrinsic carbon materials (4.1 eV) as previously reported [8]. The lower Eg value of the prepared C-dots can be assigned to the presence of different polar functional groups, which facilitated the electron transition from the valence band to the conduction band. The photoluminescence (PL) spectra of the C-dots at different excitation wavelengths ranging from 250 to 430 nm are presented in (Fig. 3**b**). The prepared nanomaterial exhibited excitation-dependent emission characteristics of typical C-dots. The excitation-dependent behavior of C-dots can be attributed to multi-emission centers, delay in solvent relaxation, nanomaterial size distribution, and multiple aggregations. Interestingly, a red shift and decrease in the intensity of the emission wavelength occurred with increasing the excitation wavelength. The excitation-dependent and red-shifting characteristics of C-dots have significant advantages in multi-color imaging applications. The normalized excitation-dependent emission spectra of the synthesized C-dots are shown in the inset of (Fig. 3**b**). The emission wavelength shift was 443 nm → 494 nm. Nanomaterials having long emissive wavelengths with good fluorescence intensity are considered attractive materials for imaging applications owing to the in-depth penetration and non-requirement of harmful UV light for excitation. The cytotoxicity of the C-dots was monitored using HDF cells after 24 h of incubation at different concentrations, and the results are given in (Fig. 4**a**). The C-dots have no adverse effects on HDF cells viability even at a higher concentration (150 μg/mL), showing good biocompatibility. This finding indicated that the developed material is sufficiently biocompatible and safe for bioimaging and other potential applications. We further conducted the cellular imaging experiment using the material to validate its utility as biocompatible nanoprobes, and the images are shown in (Fig. 4**b**). The cells were pre-labeled with cell tracker green dye (DiO) to visualize under fluorescence microscope easily. Initially (15 min), the fluorescence intensity of the dye was high compared to the C-dots showing green fluorescence morphology. However, after certain periods (60 min), the intensity of the C-dots became more prominent compared to the dye due to the sufficient intake of the C-dots inside the cells. Thus, the C-dots have the potential to be used as non-invasive nanoprobes for cellular imaging.

4. Conclusion

Herein, we synthesized value-added biocompatible nanoprobes from waste banana peels through heat treatment. The C-dots showed a negative surface charge characteristic and were solubilized in water. The C-dots showed excitation-dependent emission characteristics. The c-dots had no adverse effects on HDF cells, were easily visualized under a fluorescence microscope and could be explored as non-invasive nanoprobes for bioimaging applications.

CRediT authorship contribution statement

Dinesh K. Patel: Conceptualization, Data curation, Formal analysis, Methodology, Writing – original draft, Writing – review & editing. **So-Yeon Won:** Formal analysis. **Eunseo Jung:** Formal analysis. **Sayan Deb Dutta:** Data curation. **Tejal V. Patil:** Formal analysis, Visualization. **Ki-Taek Lim:** Visualization. **Sung Soo Han:** Funding acquisition, Project administration.

Declaration of competing interest

The authors declare that they have no known competing financial interests or personal relationships that could have appeared to influence the work reported in this paper.

Data availability

Data will be made available on request.

Acknowledgment

This research is supported by the NRF-Korea (2020R1A6A1A03044512).

Appendix A. Supplementary data

Supplementary data to this article can be found online at https://doi.org/10.1016/j.matlet.2024.136152.

References

[1] W. Su, H. Wu, H. Xu, Y. Zhang, Y. Li, X. Li, L. Fan, Mater. Chem. Front. 4 (2020) 821–836.
[2] Q. Liu, N. Zhang, H. Shi, W. Ji, X. Guo, W. Yuan, Q. Hu, New J. Chem. 42 (2018) 3097–3101.
[3] J. Chen, J.B. Luo, M.Y. Hu, J. Zhou, C.Z. Huang, H. Liu, Adv. Funct. Mater. 33 (2022).
[4] M. Feng, Y. Wang, B. He, X. Chen, J. Sun, ACS Appl. Nano Mater. 5 (2022) 7502–7511.
[5] Y. Xian, K. Li, Adv. Mater. 34 (2022).
[6] R. Atchudan, T.N.J.I. Edison, S. Perumal, N. Muthuchamy, Y.R. Lee, Fuel 275 (2020).
[7] Y. Deng, M. Chen, G. Chen, W. Zou, Y. Zhao, H. Zhang, Q. Zhao, ACS Omega 6 (2021) 4247–4254.
[8] J. Yu, C. Liu, K. Yuan, Z. Lu, Y. Cheng, L. Li, X. Zhang, P. Jin, F. Meng, H. Liu, Nanomaterials 8 (2018).